Decoupled MEMS Vibrating Gyroscope Simulations Based on Finite Element Method

Jacek Nazdrowicz

***Abstract*—In this paper the analysis of a MEMS vibrating gyroscope model is presented. The FEM analysis of the 3D structure has been performed in COMSOL Multiphysics software. Author took particular attention on mechanical properties particular parts of this device especially combs (used in electrostatical actuators and sensors) in drive and sense directions. For further electrostatic analysis (which is not covered in this article) this analysis has enormous meaning because any deformation of comb structure during operation influences on quality of electrostatic actuating and sensing. In this paper author performed stress results and deformation analysis in sense direction, however similar conclusions one can be drawn for drive direction.**

***Index Terms*—gyroscope, comb structure, MEMS, Finite Element Method.**

I. Introduction

AMONG many types of sensors criteria of size directly impacts on its application. Nowadays there are trends to miniaturize commercial products because of their comfortability ease-to-integrate with other types of devices. Microsensors and microactuators are the most developing branches of modern electronics [1-3]. Although unit cost final product in mass commercial production is relatively small, one has to remember that prototype creation takes much money, time and efforts. One has to arrange intellectual potential, advanced knowledge and advanced mathematical and numerical tools supported with IT infrastructure. This merge allows to solve complicated mathematical models applied into physical phenomena. Modeling allows to avoid cost of experiments based on physical created devices, time consuming data collection and their analysis. As a common rule, anything that is ever built must be designed first, modeling techniques and tools enable analysis to be faster and creativity of the designer is still the most important factor of whole process. Modeling techniques and tools enable analysis of an existing design which are enormously dependent on the knowledge, experience and, of course, creativity of human.

In general, there are many various structures of motion sensors [1-8] which differs with shapes and way of operation.

J. Nazdrowicz is with the Department of Microelectronics and Computer Science, Lodz University of Technology, Lodz, Poland (e-mail: jnazdrowicz@dmcs.pl).

Results presented in the paper are supported by the project STRATEGMED 2/266299/19NCBR/2016 funded by The National Centre for Research and Development in Poland.

II. Gyroscope Principle of Operation

Principle of operation MEMS capacitive gyroscope is very simple. This device consists of mass proof hanged on springs anchored to substrate. This mass includes also movable fingers extruding from all 4 sides of it [7-8]. This is moving part of whole device understood as mass-spring-damper system [9]. In sense direction comb drive structure loaded with voltage, allows to detect capacitance changes in time which in turn can be transformed into classical physics quantity [10].

Principle of gyroscope operation is based on Coriolis effect which appears in rotating objects (Fig. 1).

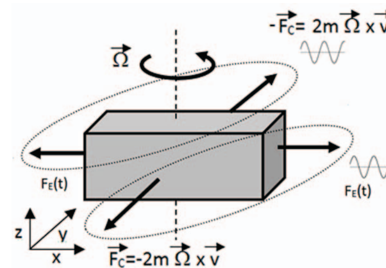

Fig. 1. Gyroscope operation principal.

During object rotation around z axis and with additionally accompanying motion along x axis additional Coriolis force appears which equals [1, 3]:

$$F_C = -2m(\vec{\Omega} \times \vec{v}) \tag{1}$$

where Ω is angular velocity, v – linear velocity, m – mass of object.

The mathematical model describing dynamics of any motion system is presented with second order differential equation which has following form:

$$ma_x = m\frac{d^2x}{dt^2} + b\frac{dx}{dt} + kx - F_{el} \tag{2}$$

where k - spring constant, b - damping coefficient, m – proof mass, x - displacement.

The equation (2) is applied in both MEMS motion sensors: accelerometer and gyroscope. Accelerometer is described by jut equation (2), gyroscope however requires application two such equations: one representing drive direction and one representing sense direction. These equations have the following form:

 Copyright © 2018 by Department of Microelectronics & Computer Science, Lodz University of Technology

$$m\frac{d^2x}{dt^2}+b_x\frac{dx}{dt}+k_x x=F_D\sin(\omega t) \tag{3}$$

$$m\frac{d^2y}{dt^2}+b_y\frac{dy}{dt}+k_y y=-2m\frac{dx}{dt}\Omega \tag{4}$$

where: m – vibrating mass, b_x, b_y – damping coefficient, k_x, k_y – spring coefficient, Ω – measured angular velocity, F_D – force generated by comb drive actuator.

Because appearance Coriolis force requires existence linear velocity, what not always is guarantee (for example in case object rotates only) – it must be enforced. Therefore artificial vibrating linear motion is enforced by actuator.

III. Gyroscope Geometry Elements

3D model of MEMS Gyroscope created in COMSOL software is fully parametrized (Fig. 2). First of were created structures like (Fig. 3): inertial mass, central spring, comb spring, external comb, internal Comb.

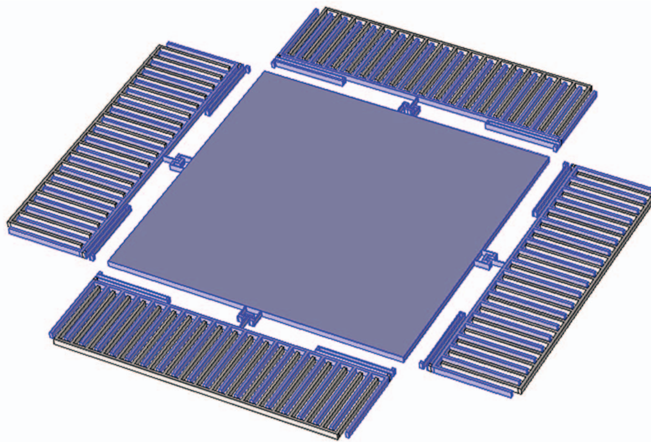

Fig. 2. General view of MEMS gyroscope considered in this article.

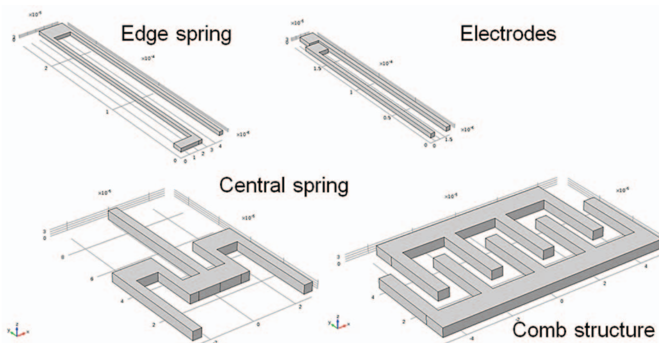

Fig. 3. Subparts of MEMS gyroscope model.

All these subparts have their local parameters which are expressed globally. This allows placement independently each object of given class with their own parameters set. Moreover model allows add new subparts (also created on these from Fig. 3 basis), what creates good, flexible environment for further creation and simulation various vibrating MEMS gyroscope structures).

Because of electrostatically requirements, this model allows to adjust width and length of inertial mass separately. This allows obtaining more space for specified direction for comb structures and this way to obtain better external force parameters or better sensitivity while keeping mass unchanged. In case of this model either drive or sense direction subparts are parametrized separately.

This model consists of inertial mass located in center and 4 comb structures located on side for both directions (Fig. 4). Motion of inertial mass causes motion of internal combs. Centered springs transfer force from drive combs to mass and from mass to combs with additional force component comes from rotation (Coriolis force). Springs located on the edges of internal combs gives elasticity to whole mass-combs system and allowing to avoid unnecessary perpendicular motions ensuring parallel orientation static and movable electrodes; this is required for keeping precision of comb electrostatic subsystems motion in both directions.

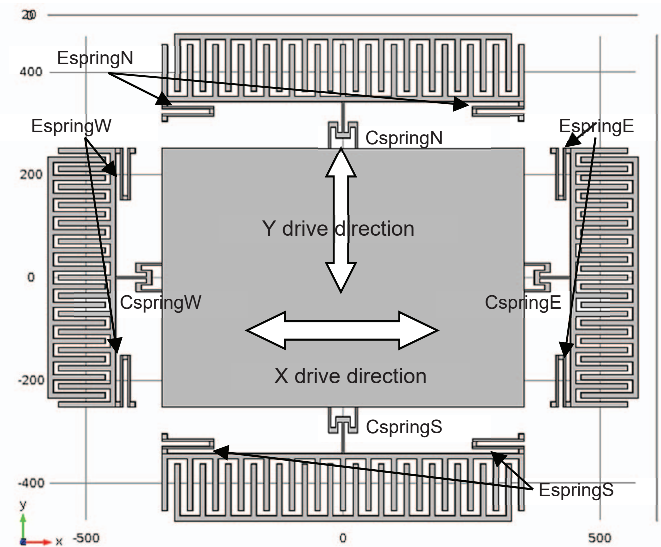

Fig. 4. Particular springs of MEMS gyroscope model and their labels.

When comb drives generate sinusoidal force along X drive direction it causes periodical motion. CspringW and CSpringE transfers force to proof mass (notice, that along X drive direction CspringW and CspringE are stiff). CspringN and CspringS deflect because along X direction they are flexible. To avoid twisting internal sense comb drives EspringNs and EspringSs prevents such motion. When object rotates, Coriolis force causes motion along sense direction. CspringNs and CspringS transfers this force to internal comb drives, and allows to move along Y direction without problems (see EspringNs and EspringSs shapes). Briefly speaking, such system of central and edge springs eliminates undesirable motions for both directions separately.

List of parameters of applied material – Polysilicon are presented in Table I. In Table II there are geometrical parameters presented.

TABLE I.
List of input parameters.

Symbol	Quantity	Value
E	Young's modulus	$169\cdot10^9$ Pa
ν	Poisson's coefficient	0.22
ρ	Density (Polysilicon)	2320 kg/m^3
a	Acceleration	1g

TABLE II.
LIST OF GEOMETRICAL PARAMETERS.

Quantity	Value
Distance between electrodes	10^{-5}m
Spring length	$250\cdot10^{-6}$m
Proof mass width	$1000\text{-}2000\cdot10^{-6}$m
Proof mass length	$1000\text{-}2000\cdot10^{-6}$m
Device thickness	10^{-5}m
Central spring length	$140\cdot10^{-6}$m
Edge spring length	$250\cdot10^{-6}$m

IV. Boundary Conditions

Because gyroscope is highly decoupled it is anchored with specific way. In Fig. 5 there is shown one side of device shown with boundary conditions.

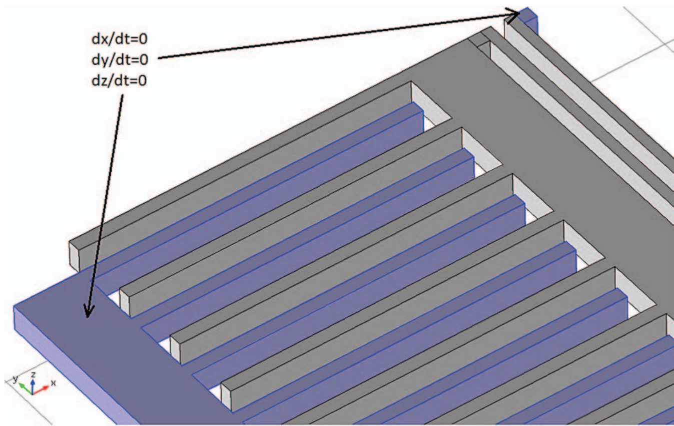

Fig. 5. Boundary conditions of MEMS gyroscope.

All remained parts can move in all directions. Force is applied to both side of movable comb. All parts are built of polysilicon which is assumed to be linear elastic material. Initial values are 0 for both displacement field and structural velocity field.

V. Meshing

Meshing has enormous meaning for simulation process. Discretization of objects in FEM is important factor which influence on duration time of simulation, therefore before this process start, it is worth to check and improve or completely change way of meshing.

In Fig. 6 we can see part of whole gyroscope object meshed automatically by COMSOL. Let’s consider area A. This is corner of inertial mass. It looks quite well, it is not necessary to improve. There is one elements layer along z axis (it is enough because mass moves in x-y plane. Moreover because of large size in compare to other part and fact that actuator will not affect directly on mass and from both sides – it is suspected that stresses on edges and corners will be the same on whole mass. Areas B and C are parts of edge spring. This is one of two kind of parts which is strained the most during operation. Edges of this kind of spring deflect meaningfully therefore mesh should be more dense there. Area D is center spring and connection between it and inertial mass. This is second type of spring stress affected the most, because beams of which spring is consisted of are thin in compare to length. Here mesh is dense enough so it is not necessary to improve it. Area E is connection between electrode and central spring. Here, again it is area with stress gradient is suspected to be high therefore mesh is dense here.

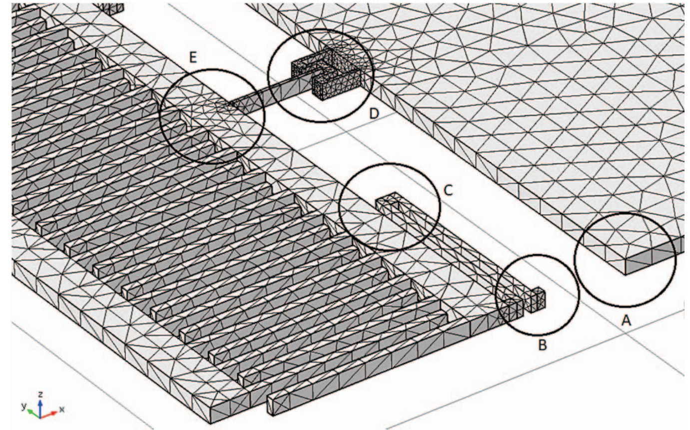

Fig. 6. Boundary conditions of MEMS gyroscope.

Because movable electrodes fingers are in the same distance form static electrodes, we can assume that they will be not deflect meaningfully, so this is not necessary to change the way of meshing (it is homogeneous).

Because this mesh should be improved in B area and because it is suspected that stress gradient is high, mesh has been modified agree to Table III.

TABLE III.
MESHING PARAMETER BEFORE AND AFTER MODIFICATIONS.

Meshing parameter	Before modification	After modification
Maximum element size	107 μm	36.4 μm
Minimum element size	40.4 μm	3.03 μm
Maximum element growth rate	1.15	1.5
Curvature factor	0.6	0.3
Resolution of narrow regions	0.7	0.95

Finally, where gradient is not high, mesh is sparse and along with gradient growth mesh gradually become dense. As we can observe tetrahedral element was used (Fig. 7).

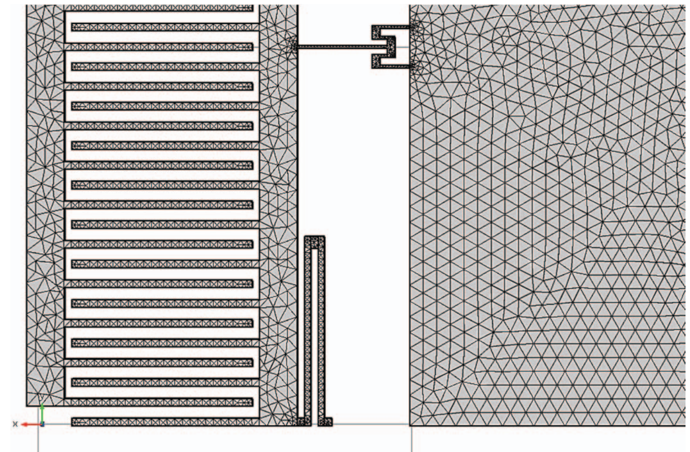

Fig. 7. Mesh after modifications.

VI. Results of Simulations

The crucial in designing process is to check and adjust geometrical dimensions so as to get acceptable measurement features and minimize undesirable motion components. Let's take a look at Fig. 8 and 9. These are example displacement and stress results for application external force in two ways: to one comb only (Fig. 8) and to both combs along X drive direction (Fig. 10). In both cases we can observe that motion and deformation of Y combs along X direction is minimized.

When we compare both cases we can observe that external forces applied on both side of drive direction is more effective (total sum of forces is the same in both scenarios), because amplitude of deformation is larger, there is better stress distribution (in case of single force application scope of stress in X drive comb - $5*10^{-9}$ N/m^2 is wider than in case of both comb force applied - $1.5*10^{-9}$ N/m^2). Moreover displacement along x axis in case of single force is 0.5µm, in case of double force applied - 0.8 µm.

In Fig. 9 and 11 there are results of comb drive deformation presented for one comb force applied (Fig. 9) and both combs force applied (Fig. 11) with scale factor: $6.9622*10^9$. Again, application on both ends force gives in results less deformation both movable combs what in results (with appropriate springs) allows keeping homogeneous field between electrodes, what is incredibly important especially in case of sense direction (influence on measurement accuracy).

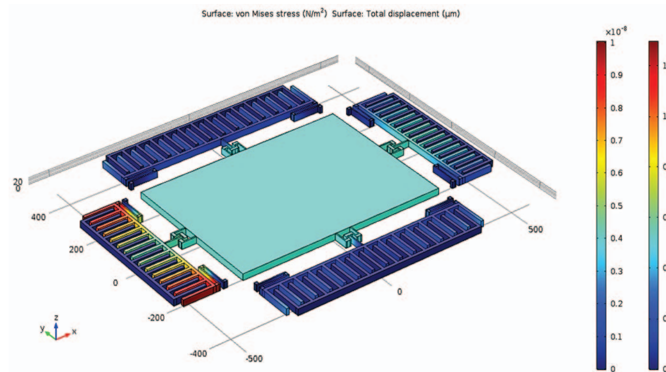

Fig. 8. Displacement and von Misses stress results for one comb force applied.

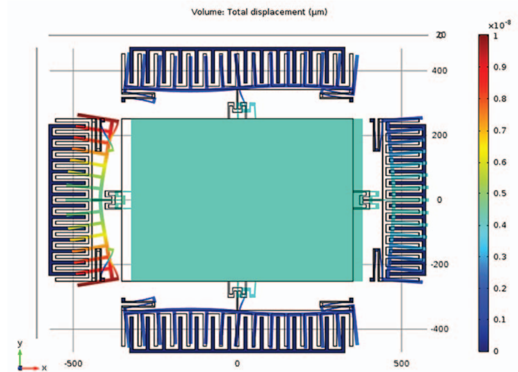

Fig. 9. Comb drive and sense deformation for one comb force applied.

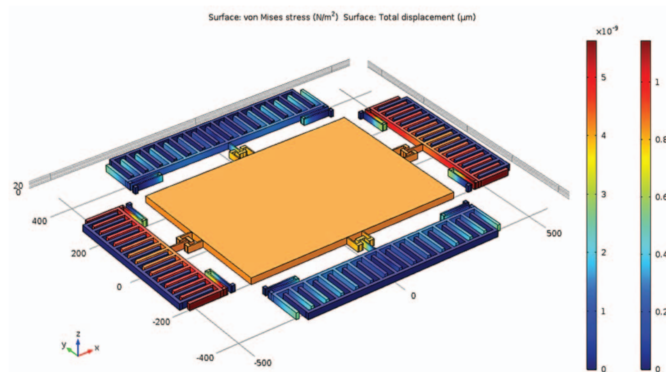

Fig. 10. Displacement and von Misses stress results for both combs force applied.

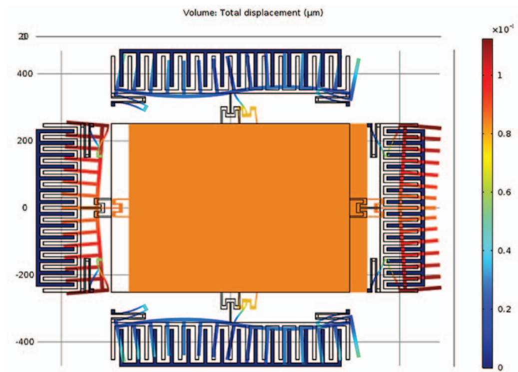

Fig. 11. Comb drive and sense deformation for both combs force applied.

Another test was performed with change spring anchors locations. In Fig. 5-8 anchors were located at both ends of combs. Then springs were moved to 0.25 of comb beam length (Fig. 12). Observing combs deformations along both directions we can see that in this case range of deformation is 1-$2.5*10^{-8}$m - in previous case – 1-$1.2*10^{-8}$m.

Obviously, this scope can be changed with change geometrical dimensions of springs, especially their length. But in such case it is necessary to consider enlarge central spring to avoid spring hit with comb and inertial mass during operation what has negative impact on drive and sense operational range.

Problem of proper placement edge springs for moving comb and optimized dimensions all component parts has meaningfully meaning for capacitance measurement. Because this is mass which has non-zero dimensions, always we need to take into consideration some mechanical behaviors of such mass resulting from material properties and physical dimensions.

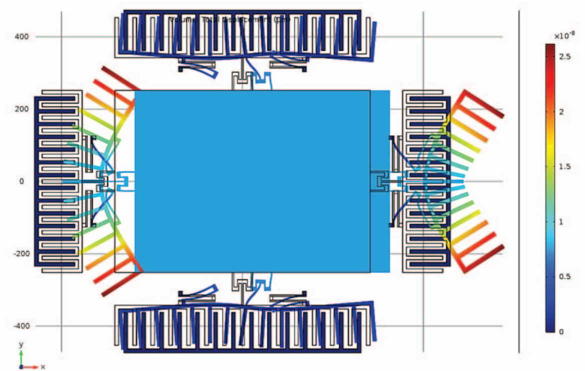

Fig. 12. Displacement results and deformations of particular comb structures under applied acceleration.

Nodes are numbered as following in Fig. 13. These labels simplify identification each of them. First simulations were

performed in 10-100[rad/s] range with 10[rad/s] step. These particular rotational velocities applied were intended to show deformations very clearly and their potential impact on measurement process. Of course for lessen velocities phenomena of deformations also exists.

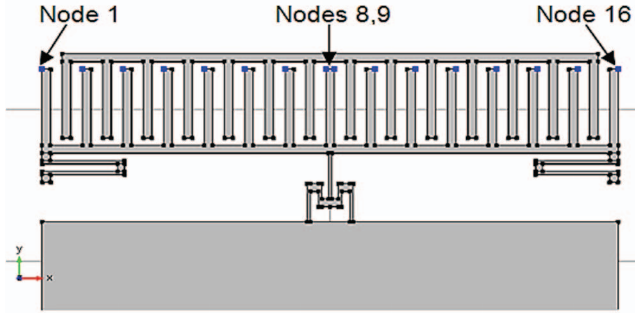

Fig. 13. Numbering of comb particular nodes.

In Fig. 14 there are results of displacement particular nodes for different rotational velocity. In all cases there is visible (especially for edge nodes) that they deform other in reference to others nodes what confirms that comb also deforms. This deformation grows along with getting away from symmetry axis which is located between node 8 and 9. For these nodes displacement is as small as can be considered as negligible.

This motion is avoided by central spring application. For each nodes set of nodes displacements grows along with rotational velocity. This dependency is non-linear what we can also see in Fig. 14.

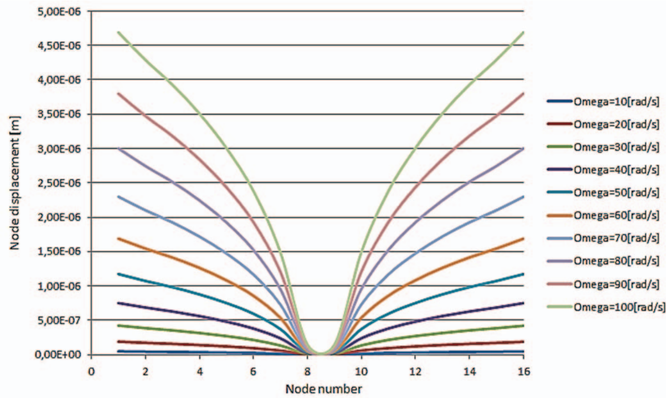

Fig. 14. Displacement of particular nodes for different rotational velocities applied.

It can be deduced that comb beam deformation problem is directly related to its thickness. For thinner beam deformation is larger - this is confirmed in Fig. 15. For thick comb beam ($50*10^{-6}$m) displacements of all nodes are very close and difference between both extreme ones is less than $1*10^{-8}$m. However for thin beam ($10*10^{-6}$m) this difference is much larger (almost 5 times more).

When we observe behavior of central spring we see that this structure moves only in one direction. This is extremely important because during rotation inertia of comb drive connected to proof mass (which has possibility to move) could change unpredictably orientation of capacitor electrodes sensor and this way upset gyroscope operation, especially capacitance measurement along sense direction.

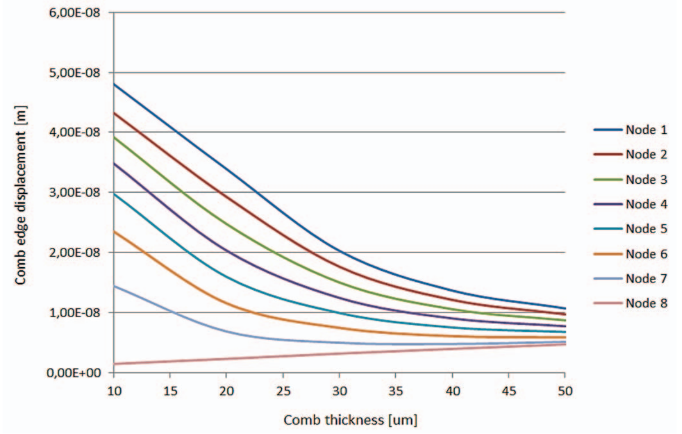

Fig. 15. Comb edge displacement for half amount of nodes (symmetry) for different comb beam thickness.

In Fig. 16 there is displacement of MEMS gyroscope along x direction. In this device configuration inertial mass is 1000x1000μm. 10N force was applied to x direction. We observe that although comb along x directions move straight, both combs in sense direction turns what is disadvantage. This is because electrodes can touch others or electrodes orientation can be difficult to measure and then transform to other quantities.

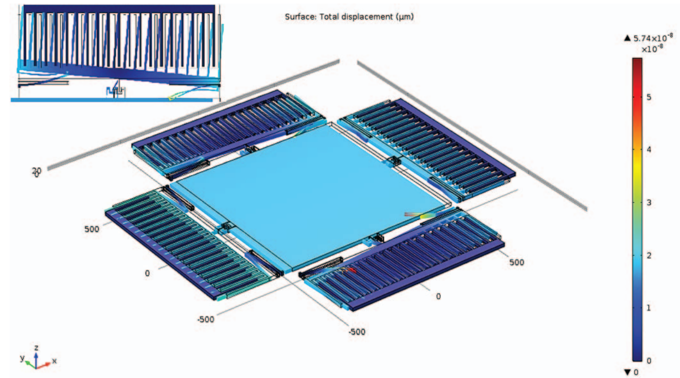

Fig. 16. Displacement along with x direction.

Because we see that deformation is meaningful in all subparts of whole device we have to consider to change some geometrical dimensions. First, central spring was modified.

Enlarging central spring from 60 μm to 120 μm with the same force loaded causes meaningful growth of amplitude in x and y directions from $3*10^{-8}$m to $8*10^{-8}$m. However comb in sense drive turns more and displacements of edges of comb drive are from - $5*10^{-8}$ to $5*10^{-8}$m. We can observe that central spring deforms meaningfuly, but both keep inertial mass stable.

Because electrode beam width was extended we do not observe meaningful deformation or unneccessary deflections. We see that this model needs to be improved with taking into consideraion movable springs.

It is worth to consider what will happen when width of edge springs will change. In fig. 18 there are results presented for doubled particular subparts of springs width. Before modification width was 4 μm and 8 μm, after - 8 μm and 16 μm respectively. We observe in fig. 18 that comb in sense direction do not rotate meaningfully around z axis (what we can see agree

to legend colors). However displacement comb in drive direction with these geometrical parameters is two times less (drops from 8.46 μm to 4.23 μm) than in case of thick comb drive – fig. 17. This fact, agree to Coriolis phenomena, will affect sense direction comb displacement (performance drops). Because of central spring dimensions (small width of particular parts), mass do not reach the same displacement as combs. This fact should be taken into consideration, because inertia can have destructive leverage on performance of the device.

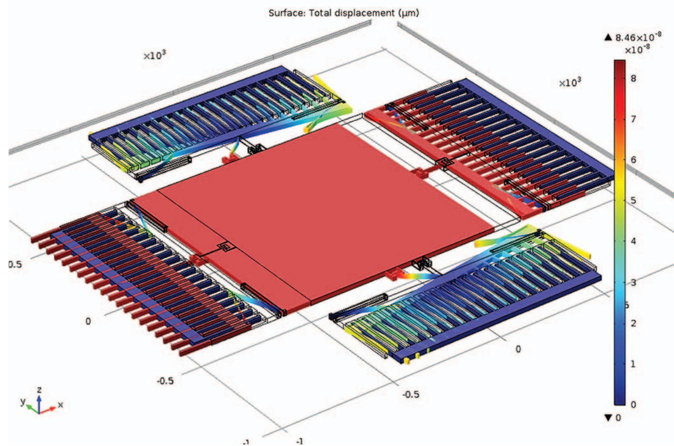

Fig. 17. Displacement along with x direction for thick comb drive.

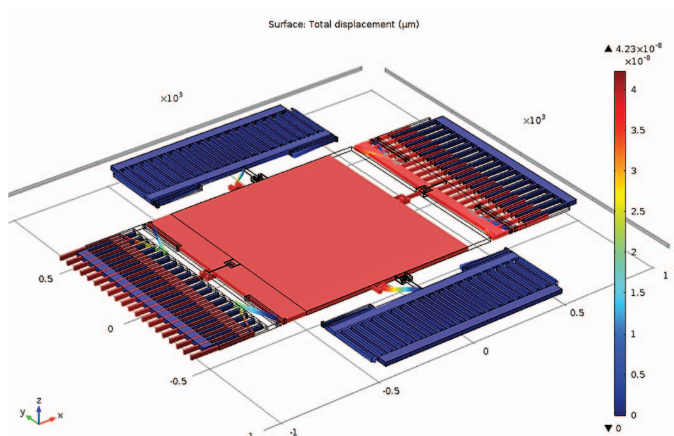

Fig. 18. Displacement along with x direction for thick edge springs.

VII. CONCLUSIONS

We need to remember that increasing comb beam dimensions causes increasing total mass of whole moving part and thus increase resonant frequency (what is extremely important value). This is because it requires to tune frequency of vibrating external force to obtain as much as possible displacement in sense direction (remembering that it is much smaller than for drive direction).

Obviously, edge springs fixed on comb beam are very helpful to stabilize motion along particular directions, but we must be aware that all of them participate in inertial motion caused by centrifugal force generated by rotational motion. Looking at behavior (deformation) moving comb MEMS gyroscope, designer is especially obligated to properly adjust geometrical dimensions of particular parts to fulfill any expectations.

The main conclusion of this paper is that gyroscope designers should clearly adjust geometrical dimensions of moving parts to separate both motion directions during operation (drive and sense) to avoid undesirably mutual impact both perpendicular forces. Moreover identified in this paper subparts which are the most stress and deformation affected should be particularly taken into consideration.

This geometry seems to be optimal, but it is worth to consider whether to apply more central and edge springs with different dimensions (and therefore different spring constant) which will keep beam stressed as less as possible.

Here, some modification were performed in this material to show what parts of gyroscope has influence on its response and what are potential solutions to minimize unnecessary influence on results.

REFERENCES

[1] https://technology.ihs.com/572622/mems-market-tracker-h1-2016

[2] M. Mehregany and S. Roy, Introduction to MEMS, Microengineering Aerospace Systems, Ed: H. Helvajian, Aerospace Press, Los Angeles, CA, USA, 1999.

[3] N. Yazdi et al., Micromachined inertial sensors, Proceedings of the IEEE, vol. 86, pp. 1640-1659, 1998.

[4] N. Maluf, K. Williams, An Introduction to MicroElectromechanical Systems Engineering, 2th ed Artech House Inc., pp. 79-131, 2004.

[5] S. E. Lyshveski, MEMS and NEMS: Systems, Devices and Structures, CRC Press, pp. 109-136, 2002.

[6] T. Smith, A 15b Electromechanical Sigma-Delta Converter for Acceleration Measurements, in Proc. of IEEE Int. Solid-State Circuits Conf. Digest of Technical Papers, pp. 160-161, San Francisco, CA, 1994.

[7] A. Lawrence, Modern Inertial Technology: Navigation, Guidance and Control, .Springer Verlag, New York,1993.

[8] V. Kempe, Inertial MEMS: Principles and Practice, Cambridge University Press, pp. 227-282, 2011.

[9] G. Zhang, Sensing and Control Electronics for Low-Mass Low-Capacitance MEMS Accelerometer, *Ph.D. Dissertation*, Carnegie Mellon University, 2002, https://www.ece.cmu.edu/~mems/pubs/pdfs/ece/phd_thesis/0201_wu-2002.pdf.

[10] L. Zimmermann, J. Ebersohl, F. Le Hung, J. P. Berry, F. Baillieu, P. Rey, B. Diem, S. Renard, P. Caillat, Airbag application: a microsystem including a silicon capacitive accelerometer, CMOS switched capacitor electronics and true self-test capability. Sensors and Actuators, pp. 190-195, 1995.

Jacek Nazdrowicz was born in Poddębice, Poland, in 1975. He received the MSc degrees in Technical Physics (Computer Physics), Computer Sciences (Software Engineering and Networking Systems), Marketing and Management, Mathematics from the Lodz University of Technology, Poland, in 2001, 2002, 2004 and 2018 respectively and the PhD degree in Economics Sciences, Management discipline, in Lodz University of Technology, in 2013.

From 2014 he attends doctoral study in Lodz University of Technology, electronics discipline. His research interests include modelling and simulation MEMS devices and their application in medicine. He participated in EduMEMS project (Developing Multidomain MEMS Models for Educational Purposes). He also educates in COMSOL software. Now he participates in Strategmed project (supported by the National Center for Research and Development)

Between 2007 and 2016 he worked in mBank as a System Engineer of SQL Server databases. He has the following certifications: MCSA Windows 2012, MS SQL Server 2012 and Storage Area Network (SAN) Specialist.

Since 2016 he also works in Fujitsu Technology Solutions in Lodz in Remote Infrastructure Management Department in Storage Team as a Storage Engineer (SAN Infastructure, Brocade, Netapp, Eternus products). He educates in many data storage and backup technologies (IBM, DELL/EMC, Hitachi, Fujitsu).